Fracture Toughness Estimation of Thin Chemical Vapor Deposition Diamond Films Based on the Spontaneous Fracture Behavior on Quartz Glass Substrates

doi: 10.1063/1.366473

Fracture toughness estimation of thin chemical vapor deposition diamond films based on the spontaneous fracture behavior on quartz glass substrates

Shoji Kamiya, Masaki Sato, and Masumi Saka
Department of Mechanical Engineering, Tohoku University, Aramaki aza Aoba, Aoba-ku, Sendai 980-77, Japan

Hiroyuki Abé
Tohoku University, 2-1-1 Katahira, Aoba-ku, Sendai 980-77, Japan

(Received 9 June 1997; accepted for publication 9 September 1997)

This article is on the experimental estimation of the fracture toughness of thin diamond film deposited by the microwave plasma chemical vapor deposition method on a quartz glass substrate. Because of their differences in the coefficient of thermal expansion, diamond films on a quartz glass substrate suffer tensile stress at room temperature and show various kinds of spontaneous fracture behavior, reflecting the mechanical properties of the films. On the basis of detailed observation of cracking patterns and also measuring the residual stress with the aid of Raman spectroscopy, the fracture toughness of the film having thickness of around 1 μm has been estimated here satisfactorily without the help of any difficult microscopic experiment. The fracture toughness of the film of thickness 0.35 μm is found to be around half of that obtained with much thicker films. [S0021-8979(97)02224-X]

I. INTRODUCTION

The synthetic polycrystalline diamond films produced by chemical vapor deposition (CVD) onto the substrates are being used for many applications due to their extreme properties,[1–3] for example, the highest hardness, stiffness, thermal conductivity at room temperature, and also good corrosion resistance. In addition, diamond film is also expected to be used as a new semiconductor material, especially for the high temperature environment.[4]

For the practical use of CVD diamond films, an engineering parameter of interest, the resistance to fracture as characterized by fracture toughness, is of great importance, in order to ensure their mechanical integrity. Drory *et al.*[5] measured the fracture toughness of relatively thick CVD diamond film of thickness 150–200 μm by conventional compact tension specimens and also by Vickers indentation technique. In the case of thinner diamond films, microscopic cantilevers of 15–28 μm thickness were broken in a scanning electron microscope and their ultimate tensile strength was reported by Hollman *et al.*[6] Burst pressure technique[7,8] was also utilized for the diamond films of various thicknesses ranging from 1 to around 150 μm, where the critical pressure required to explode circular disks of the films was measured to evaluate the fracture strength. In these reports, they succeeded in carrying out conventional fracture tests with small scales by applying a mechanical load to the specimens made of free standing films without substrates. However, these methods of direct measurement come up with extreme difficulties for the cases of extremely thin films. Mecholsky *et al.*[9] carried out indentation tests on 6- and 12 μm-thick CVD diamond films on a silicon substrate to examine the fracture toughness. Although they reported the apparent fracture toughness of silicon coated with diamond, the individual fracture toughness of diamond films was not obtained since the indentation cracks always penetrated the interface.

Accordingly, the objective of this article is to evaluate the fracture toughness of thin CVD diamond films of thickness less than 1 μm, which has not been estimated yet. With such a small film thickness, it would be practically impossible to carry out the conventional fracture toughness tests by preparing small specimens. Quartz glass is chosen here as the substrate material on which diamond was deposited to form the film. Since quartz glass has the coefficient of thermal expansion lower than that of diamond, the diamond films on a quartz glass substrate suffer tensile stress at room temperature and show various kinds of spontaneous fracture behavior in which mechanical properties of films are reflected. On the basis of detailed observation of cracking patterns, the fracture toughness of diamond films is successfully obtained without the aid of any difficult microscopic experiment.

II. EXPERIMENTAL OBSERVATION

A. Chemical vapor deposition of diamond on the quartz glass substrate

We prepared the substrates made of quartz glass with the dimension of $12.5\times12.5\times2$ mm. Prior to deposition, the substrates were lightly scratched with the help of 2 μm diamond powder in order to enhance the diamond nucleation, and rinsed in water. Diamond growth was obtained in a microwave plasma reactor at the excitation frequency of 2.45 GHz in the gas mixture of 99% hydrogen and 1% methane. The total gas flow rate was 100 sccm. Substrate temperature was controlled to be 1120 K.

In the early stage of deposition, discrete particles of diamond crystal appeared sparsely on the substrate and then grew up into contact with each other to form a continuous film within the period of slightly less than 1 h. After continu-

 0021-8979/97/82(12)/6056/6/$10.00

TABLE I. Film thickness of specimens.

Specimen No.	Film thickness t_f μm
1	0.35
2	0.78
3	1.78
4	2.50

ous deposition for 1–6 h, we obtained four specimens with different film thickness as indicated in Table I. The actual film thickness was measured by a laser scanning microscope as the difference in level where a part of the film was compulsorily scratched off. Note that a film thickness of 0.35 μm, as in the case of specimen No. 1, is almost the minimum thickness where diamond particles could form a continuous film.

During cooling down from deposition to room temperature, the misfit of shrinkage between diamond films and quartz glass substrates results in residual tensile strain in diamond films. According to the reported thermal expansion coefficients of diamond[10] and quartz glass,[11] as presented in Fig. 1, we estimated the residual tensile strain to be about 2.3×10^{-3}. Spontaneous fracture of diamond films takes place due to this tensile strain, which will be presented in the next section.

B. Appearance of spontaneous fracture

Figure 2 shows the state of spontaneous fracture that appeared in the specimens. Figure 2(a) is the photo of specimen No. 1 taken at room temperature. Cracks in the film can be observed on the whole specimen surface, as are emphasized in the circle, and the cross section of the film cracks is schematically illustrated in Fig. 3(a). On the other hand, Fig. 2(b) represents the photograph of specimen No. 3, where two different kinds of fracture on the specimen surface are observed. One is the film cracks shown in region B enclosed with a white line in Fig. 2(b), which is the same as those observed in specimen No. 1. Another is found in region A shown in the same figure, where film cracks extend into the

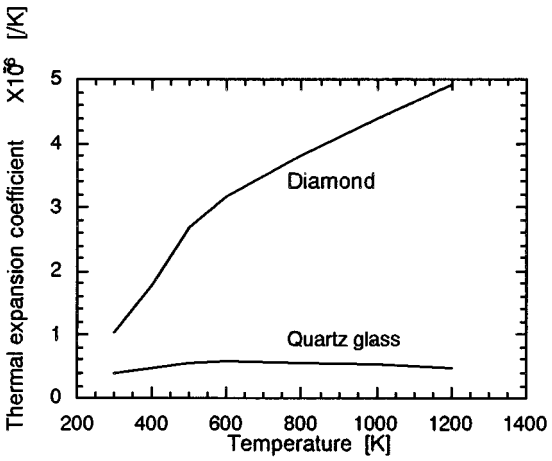

FIG. 1. Thermal expansion coefficients of quartz glass and diamond.

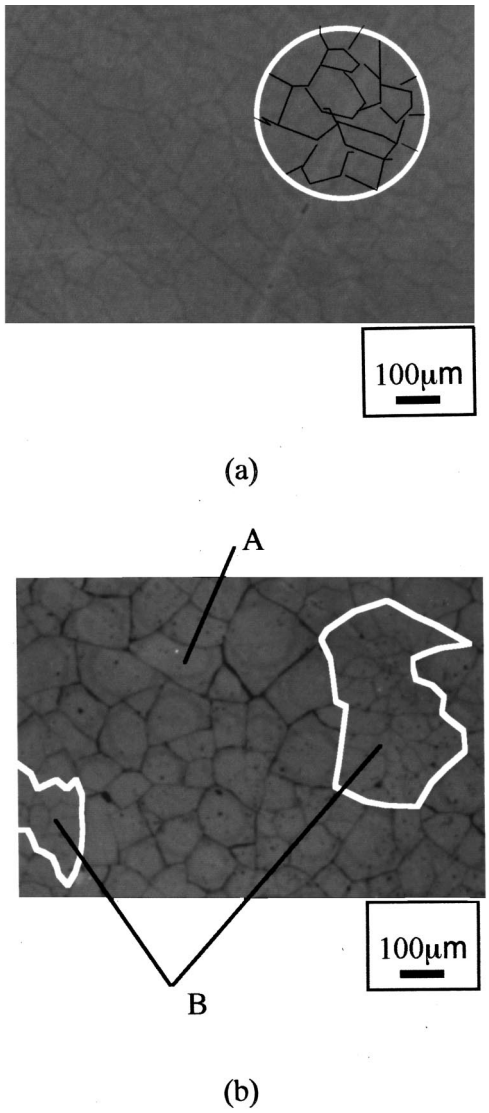

FIG. 2. Typical appearance of diamond film on quartz glass substrate: (a) specimen No. 1 ($t_f=0.35$ μm) and (b) specimen No. 3 ($t_f=1.78$ μm).

substrate and are bent in the direction parallel to the surface, as illustrated in Fig. 3(b). These cracks are usually called as spalling cracks.[12] These characteristic situations of damage were revealed in detail by the observation performed from the backside of specimens using a microscope. As can be seen in Fig. 3(b), region B, emphasized with a white line, appears as the islands surrounded by the ocean of region A, which would be a distinctive feature of this material system. We have to write in addition that the interface delamination between the film and substrate is not found in all the four specimens.

The areal percentage of region A actually increases with film thickness. The whole area is covered with region B in the case of specimen No. 1, i.e., no spalling crack appears, while the surface of the specimen No. 4 is totally occupied with region A, i.e., all the cracks are spalling cracks.

C. Progress of fracture during cooling process

Based on the results observed in the previous section, the progress of spontaneous fracture during the cooling process

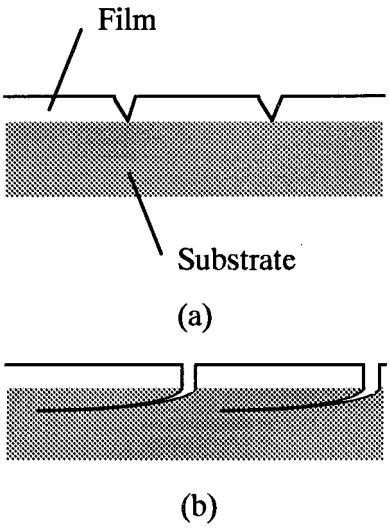

FIG. 3. Schematic illustrations of the cross sections of specimens with cracks: (a) film cracks and (b) spalling cracks.

is considered, as illustrated schematically in Fig. 4. At the deposition temperature, no damage is supposed in the specimen, as shown in Fig. 4(a). While temperature comes down, tensile thermal stress gradually increases and at first causes the film cracks, as illustrated in Fig. 4(b). In the cases of extremely thin films, other forms of fracture do not occur until getting to the room temperature because of the fact that only a little energy is stored in the film. However, with larger film thicknesses, cracks proceed into the substrate and extend parallel to the surface, thereby leading to the spalling cracks.

Here let us suppose that all the spalling cracks around a region extend in the direction away from that region, as illustrated in Fig. 4(c). Then the film in that region, say region B, as indicated in Fig. 4(c), is separated from the surrounding region A, which results in relaxation of residual stress in region B. When the temperature goes further down, film cracks take place inside region B, as shown in Fig. 4(d). However, due to the stress relaxation caused by the surrounding spalling cracks in region A, these film cracks in region B cannot penetrate the interface any more until reaching room temperature. Hence, two forms of fracture are observed simultaneously in one specimen, as shown in Fig. 2(b), where the islands of region B are surrounded by the ocean of region A.

III. ESTIMATION PROCEDURE OF ENERGY RELEASE RATE

Now we focus our attention to the spacing of film cracks in region B. The fracture toughness of diamond films can be evaluated by calculating the amount of energy released during the extension of film cracks, which is discussed in the following.

Suppose that the film without any crack has the uniform residual stress, σ_T, caused by the deposition and subsequent cooling. When a crack extends in the film, stress in the neighborhood of the crack surfaces is relaxed and a part of strain energy stored in the film is released.[12] Figure 5(a) shows the cross section with the film cracks, and in the lower

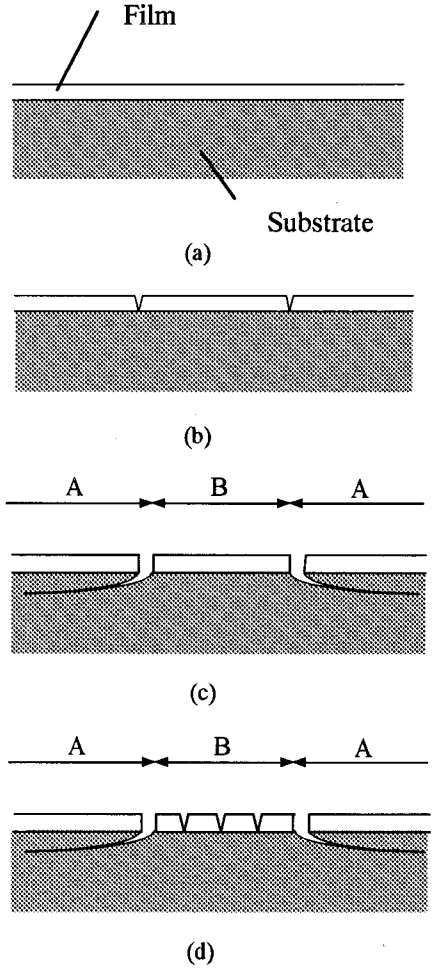

FIG. 4. Schematic illustrations of the progress of spontaneous fracture during the cooling process: (a) no crack observed at diamond deposition temperature, then (b) film cracks appear, (c) spalling cracks in region A, and (d) subsequent film cracks in region B.

side of the figure the distribution of relaxed stress in the film is schematically illustrated, by which the resulting state of energy can easily be calculated. However, it is worth noting that the amount of energy released per one crack decreases with increasing density of cracks. Hence, we can obtain the critical energy release rate of the film, which represents the energy required to produce the unit area of crack surface and is equivalent to the fracture toughness, by measuring the average crack spacing d in Fig. 5(a), provided that the original residual stress, σ_T, can be estimated.

In case the specimen contains only film cracks, σ_T simply means the total residual stress generated in the process of deposition and subsequent cooling to room temperature. However, in the actual specimens, region A with spalling cracks appears in addition to region B with film cracks, as shown in Fig. 2(b). Therefore we need to estimate how much the residual stress relaxes in region B due to the existence of region A. Since spalling cracks scrape off the surface of glass substrates by several microns, for example, around 5 μm in the case of specimen No. 3, region A could be supposed to be mechanically equivalent to the bare substrate surface without the film for the stress relaxation in region B. A computational model is set up, where the film in region A

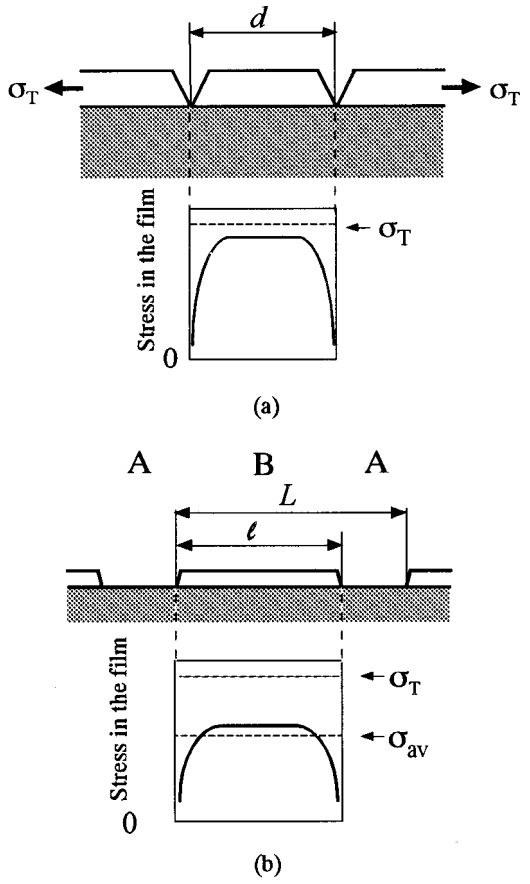

FIG. 5. Stress relaxation caused by film cracks (a) and spalling cracks (b).

is removed, as shown in Fig. 5(b). By using this model, the distribution of residual stress relaxed by region A can be calculated with the actual dimension of region B and its spacing, i.e., l and L as designated in Fig. 5(b), respectively. Note that the model in Fig. 5(b) has no film cracks in region B. For the evaluation of energy release rate with respect to the film crack extension in region B surrounded by region A, σ_T in the previous discussion should be simply replaced by the average of the relaxed stress distribution, σ_{av}, as indicated in Fig. 5(b).

We actually measured the average size and spacing of region B and crack spacing in region B designated as l, L, and d in Fig. 5, respectively. Table II shows the actual region B data, where the upper number indicates the average and the lower number in parentheses means the standard deviation for each dimension. Then, the deformation of cross sections of specimens was analyzed by using the finite element

TABLE II. Average and standard deviation of size and spacing of region B, and crack spacing in region B.

Specimen No.	l	L	d [μm]
1	···	···	51.60 (5.88)
2	449.40 (83.47)	471.21 (94.63)	79.37 (17.45)
3	348.33 (105.26)	841.22 (172.18)	53.19 (16.76)

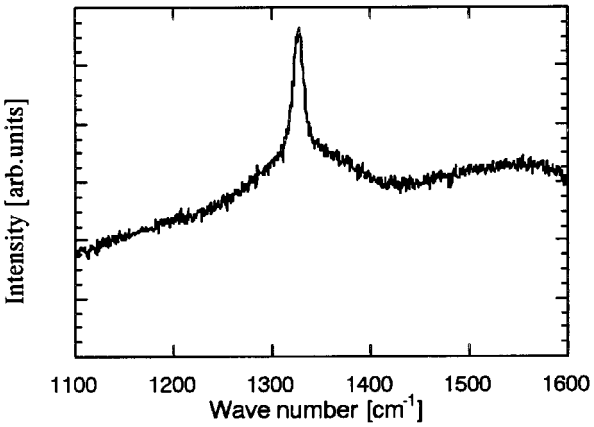

FIG. 6. Raman spectrum from the specimen No. 1.

method. Although films are thin, their cross sections with substrates should be treated as two-dimensional problems under the condition of plane strain.[12] In this way, we estimate the critical energy release rate of film cracks in region B.

IV. MEASUREMENT OF RESIDUAL STRESS

In order to execute the calculation in the discussion above, it we needed to know about the original residual stress, σ_T, and the elastic moduli of the film.

The residual strain was measured by performing micro-Raman spectroscopy on the diamond film. Raman spectrum obtained from specimen No. 1 is shown in Fig. 6. Although stress free diamond is known to have a peak located at 1332 cm^{-1} in its Raman spectrum, a distinctive peak is observed at 1329 cm^{-1} in Fig. 6. This shift is caused by residual strain in the lattice of diamond crystal and corresponds to the tensile in-plane biaxial strain $\epsilon_c = 1.6 \times 10^{-3}$ according to Ager *et al.*[13] This amount of strain is a little smaller than what we estimated from the difference in the coefficient of thermal expansion. Since the peak shift in Raman spectrum means the strain of diamond crystal itself, we can obtain the stress, σ, in the film by operating the elastic moduli of diamond crystal as in the following equation:

$$\sigma = E_c' \epsilon_c , \tag{1}$$

where E_c' means the biaxial modulus defined as

$$E_c' = \frac{E_c}{1-\nu_c} . \tag{2}$$

In Eq. (2), E_c and ν_c represent Young's modulus and Poisson's ratio of diamond crystal, respectively, which are reported[13,14] to be 1050 GPa and 0.07. Hence, 1.8 GPa of tensile stress can be obtained as the measured value of residual stress in the case of specimen No. 1.

Note that the stress we measured above would be the average stress in the diamond film on specimen No. 1, which was already relaxed with film cracks. Hence, in order to obtain the original stress σ_T, measured stress is divided by the ratio, called here the average stress relaxation ratio. The average stress relaxation ratio in specimen No. 1 represents the

average of residual stress relaxed by film cracks and is obtained by calculating the stress distribution using the finite element method. This calculation of course needs the elastic moduli of the films.

Now let us focus our attention on the curvature of spalling flakes. Spalling flakes consists of the films adhered to thin substrates produced by the extension of spalling cracks as we discussed in the foregoing section. Equilibrium of bending moment and in-plane stress in a spalling flake lead to the following relation between the radius of curvature, R, and the original residual stress, σ_T, in the film:

$$R\sigma_T=\frac{E_s' t_s^3}{6t_f(t_f+t_s)}\left\{1+\frac{E_f' t_f}{E_s' t_s}\left[4+6\frac{t_f}{t_s}+4\left(\frac{t_f}{t_s}\right)^2+\frac{E_f'}{E_s'}\left(\frac{t_f}{t_s}\right)^4\right]\right\}, \tag{3}$$

where E_f' and E_s' are the biaxial modulus of the film and substrate, respectively. Thickness of the film in the spalling flake is denoted by t_f and that of the substrate by t_s in the above equation. Therefore, as the elastic moduli of the substrate are already known and also R can actually be measured, we can determine biaxial modulus of the film by solving Eq. (3) for E_f', if only we know the stress, σ_T.

According to the discussion above, the stress and moduli were estimated simultaneously in the following procedure. At first, we supposed moduli of the film to be equal to that of bulk crystal. With this assumption, the average stress relaxation ratio in specimen No. 1, and hence the original residual stress, were obtained by calculating the stress distribution. Next, the radius of curvature of the spalling flake obtained from specimen No. 4 was measured by a laser scanning microscope, and thus the value of the biaxial modulus of the film was estimated by solving Eq. (3). Then we set this modulus into finite element calculation and again obtain the original residual stress. By repeating this procedure, σ_T and E_f' were determined to be 2.0 and 660 GPa, respectively, and were assumed to be constant in all the four specimens. Poisson's ratio[13,14] of the film was supposed to be 0.07 throughout our calculation. The obtained value of E_f' is found to be similar to that reported by Hollman *et al.*,[6] where bending tests were performed for cantilevers made of free standing CVD diamond films with the thickness of 15–28 μm.

The average stress relaxation ratio calculated for specimen Nos. 1–3, with the moduli determined above is shown in Fig. 7. In Fig. 7, the average stress relaxation ratio represents the average of the residual stress in region B relaxed by film cracks, and spalling cracks in region A if any, normalized with respect to the original residual stress in the case of no cracks. Experimental results obtained by Raman spectroscopy are also plotted in Fig. 7, where the measured stress is normalized by the obtained value of $\sigma_T=2.0$ GPa. Calculated variation of stress relaxation ratio with respect to the specimens appears in good agreement with the experimental trend. This fact proves that our consideration about the state of deformation of films, along with the assumption of constant σ_T and constant E_f', is sufficiently appropriate.

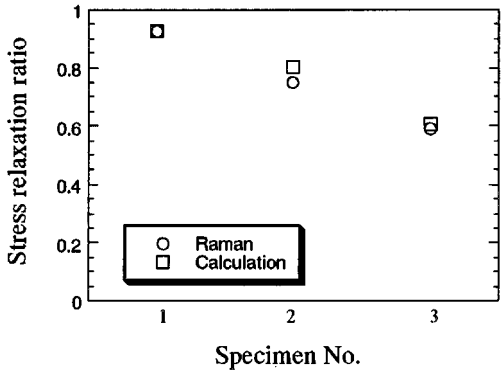

FIG. 7. Measured and calculated stress relaxation ratio.

V. ESTIMATION RESULTS OF FRACTURE TOUGHNESS

In accordance with the procedure discussed above, the critical energy release rate of the diamond films was estimated. Critical energy release rate G_c is known to be related with fracture toughness K_c by the following equation:[12]

$$K_c=\sqrt{E^* G_c}, \tag{4}$$

where

$$E^*=\frac{E_f}{1-\nu_f^2} \tag{5}$$

in the case of plane strain condition. In Eq. (5), ν_f represents Poisson's ratio of the films. Obtained values of fracture toughness for the specimen Nos. 1–3 are plotted in Fig. 8 against the corresponding thickness of the films. Fracture toughness of diamond films with the thickness of 150–200 μm reported by Drory *et al.*[5] is also presented at the right side end of Fig. 8, which was measured by using conventional compact tension specimens made of free standing diamond films. As can be seen in the figure, fracture toughness tends to increase gradually with film thickness. It is here mentioned that even though some of the standard deviations presented in Table II are up to about 30%, their influence on the estimation results of fracture toughness has been revealed to be within only a few percent. In the case of specimen No. 1, fracture toughness is estimated to be about 3 MPa $m^{1/2}$,

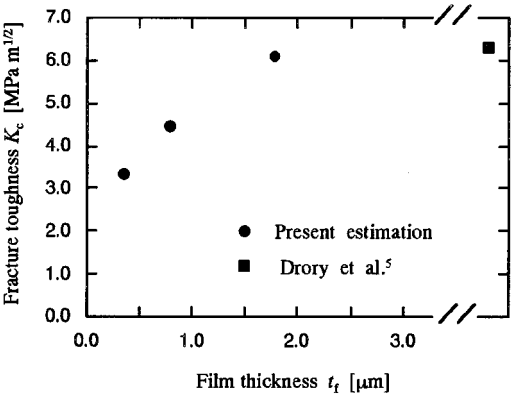

FIG. 8. Estimated results of fracture toughness.

which is only about a half of the value reported by Drory *et al.*[5] As we previously mentioned, the thickness of 0.35 μm is almost the minimum for the diamond deposited in our experiment to form a continuous film. Since CVD diamond films consist of particles of diamond crystal which come into contact with each other, extremely thin films might contain more defects which would lead to low fracture toughness.

VI. CONCLUSIONS

Fracture toughness of extremely thin diamond films produced by chemical vapor deposition was successfully estimated. Diamond films were deposited on quartz glass substrates and stressed in tension at room temperature due to the difference in their thermal expansion coefficients. On the basis of detailed observation of the appearance of spontaneous fracture in the films, the critical energy release rate of films was estimated, which was equivalent to the fracture toughness. Here, the present analysis showed that the fracture toughness would be smaller for the case of extremely thin films due to their structure, where discrete particles of diamond crystal came into contact with each other to form a continuous film in the early stage of deposition.

ACKNOWLEDGMENTS

This work was partly supported by Grant-in-Aid for Scientific Research No. (B)(2) 08455050 and Grant-in-Aid for Encouragement of Young Scientists No. 09750094 from the Ministry of Education, Science, Sports, and Culture of Japan. The authors also wish to thank Professor H. Arashi and Associate Professor H. Yugami in Tohoku University for their help in the measurement of residual stress by Raman spectroscopy.

[1] W. A. Yarbrough and R. Messier, Science **247**, 688 (1990).
[2] J. C. Angus and C. C. Hayman, Science **241**, 913 (1988).
[3] K. E. Spear, J. Am. Ceram. Soc. **72**, 171 (1989).
[4] W. P. Kang, J. L. Davidson, Y. Gurbuz, and D. V. Kerns, J. Appl. Phys. **78**, 1101 (1995).
[5] M. D. Drory, R. H. Dauskardt, A. Kant, and R. O. Ritchie, J. Appl. Phys. **78**, 3083 (1995).
[6] P. Hollman, A. Alahelisten, M. Olsson, and S. Hogmark, Thin Solid Films **270**, 137 (1995).
[7] G. F. Cardinale and C. J. Robinson, J. Mater. Res. **7**, 1432 (1992).
[8] Y. Aikawa and K. Baba, Jpn. J. Appl. Phys., Part 1 **32**, 4680 (1993).
[9] J. J. Mecholsky, Jr., and Y. L. Tsai, J. Appl. Phys. **71**, 4875 (1992).
[10] G. A. Slack and S. F. Bartram, J. Appl. Phys. **46**, 89 (1975).
[11] Toshiba Ceramics Co., Ltd., Quartz and Silica Glass Ref. No. TC086-86.04.2A.
[12] J. W. Hutchinson and Z. Suo, in *Advances in Applied Mechanics* (Academic, New York, 1992), Vol. 29, p. 63.
[13] J. W. Ager III and M. D. Drory, Phys. Rev. B **48**, 2601 (1993).
[14] M. H. Grimsditch and A. K. Ramadas, Phys. Rev. B **11**, 3139 (1975).